Published in final edited form as:

Exp Eye Res. 2017 December ; 165: 175–181. doi:10.1016/j.exer.2017.09.011.

Long-term photoreceptor rescue in two rodent models of retinitis pigmentosa by adeno-associated virus delivery of Stanniocalcin-1

Gavin W. Roddy[a], **Douglas Yasumura**[b,1], **Michael T. Matthes**[b], **Marcel V. Alavi**[b], **Sanford L. Boye**[c], **Robert H. Rosa Jr.**[d], **Michael P. Fautsch**[a], **William W. Hauswirth**[c], and **Matthew M. LaVail**[b,*]

[a]Department of Ophthalmology, Mayo Clinic, Rochester, MN, 55905

[b]Department of Ophthalmology, University of California, San Francisco, CA 94143

[c]Department of Ophthalmology, University of Florida, Gainesville, FL 32610

[d]Department of Ophthalmology, Scott & White Medical Center, Temple, TX, 76508

Abstract

Retinal degenerations, including age-related macular degeneration and the retinitis pigmentosa family of diseases, are among the leading causes of legal blindness in the United States. We previously found that Stanniocalcin-1 (STC-1) reduced photoreceptor loss in the S334ter-3 and Royal College of Surgeons rat models of retinal degeneration. The results were attributed in part to a reduction in oxidative stress. Herein, we tested the hypothesis that long-term delivery of STC-1

*Corresponding author: Matthew M. LaVail, Ph.D., Department of Ophthalmology, University of California, San Francisco, CA 94143-0730. Telephone: (415) 999-6511, mmlv@sonic.net (M. LaVail).

[1]Deceased

Current Addresses and Email Addresses: “Same address” is that given on title page.

Gavin W. Roddy, MD, PhD, same address Roddy.Gavin@mayo.edu

Douglas Yasumura†

Michael T. Matthes, PhD, same address, michael.matthes@sbcglobal.net

Marcel V. Alavi, PhD, same address, marcel.alavi@gmail.com

Sanford L. Boye, MSc same address, sboye@UFL.EDU

Robert H. Rosa, Jr., MD same address, Robert.Rosa@BSWHealth.org

Michael P. Fautsch, PhD same address, Fautsch.Michael@mayo.edu

William W. Hauswirth, PhD, same address, hauswrth@ufl.edu

Matthew M. LaVail, PhD, same address, mmlv@sonic.net

Contributions of the authors:

Gavin W. Roddy, MD, PhD, All aspects of the research; planning of the studies; analysis of data; writing the manuscript; editing the manuscript.

Douglas Yasumura† All histological and morphometric analyses.

Michael T. Matthes, PhD, All histological and morphometric analyses.

Marcel V. Alavi, PhD, ERG measurements and analyses.

Sanford L. Boye, PhD., Creation of the AAV-STC-1.

Robert H. Rosa, Jr. MD, editing of the manuscript

Michael P. Fautsch, PhD Planning of the studies, editing of the manuscript

William W. Hauswirth, PhD, Creation of the AAV-STC-1.

Matthew M. LaVail, PhD, Planning of the studies; direction and oversight of project; analysis of morphological and ERG data; editing the manuscript.

would provide therapeutic rescue in more chronic models of retinal degeneration. To achieve sustained delivery, we produced an adeno-associated virus construct (AAV) to express STC-1 (AAV-STC-1) under the control of a retinal ganglion cell targeting promoter human synapsin 1 (hSYN1). AAV-STC-1 was injected intravitreally into the P23H-1 and S334ter-4 rhodopsin transgenic rats at postnatal day 10. Tissues were collected at postnatal day 120 for confirmation of STC-1 overexpression and histologic and molecular analysis. Electroretinography (ERG) was performed in a cohort of animals at that time. Overexpression of STC-1 resulted in a significant preservation of photoreceptors as assessed by outer nuclear thickness in the P23H-1 ($P<0.05$) and the S334ter-4 ($P<0.005$) models compared to controls. Additionally, retinal function was significantly improved in the P23H-1 model with overexpressed STC-1 as assessed by ERG analysis (scotopic b-wave $P<0.005$ and photopic b-wave $P<0.05$). Microarray analysis identified common downstream gene expression changes that occurred in both models. Genes of interest based on their function were selected for validation by quantitative real time PCR and were significantly increased in the S334ter-4 model.

Keywords

Retinal degeneration; neuroprotection; stanniocalcin-1; P23H; S334ter; rhodopsin

Novel neuroprotective therapies are needed for patients with retinal degeneration (RD), including age-related macular degeneration (AMD) and the retinitis pigmentosa (RP) family of diseases, which are among the leading causes of legal and irreversible blindness in the United States. AMD and RP share clinical and pathologic features including end-stage blindness secondary to photoreceptor and/or retinal pigment epithelium (RPE) cell death. Apoptosis of photoreceptors has been shown to be a prominent feature of human AMD (Dunaief et al., 2002; Xu et al., 1996) and RP (Cottet and Schorderet, 2009; Doonan and Cotter, 2004), and is the underlying feature in many of the animal models of RD (Doonan and Cotter, 2004; Katai et al., 1999; Katai et al., 2006; Yu et al., 2004), as are oxidative stress and inflammation (Cuenca et al., 2014). Multiple therapeutic strategies have been employed to slow photoreceptor degeneration, including stem cell-based treatments, gene therapy in the form of trophic factor support, gene replacement, and delivery of various neuroprotective compounds (Scholl et al., 2016). With more than 200 different identified mutations responsible for RD, one attractive therapeutic strategy is to intervene at one or multiple downstream pathway(s) that ultimately lead to cellular death.

Stanniocalcin-1 (STC-1) is a unique multifunctional protein that is cellular protective in a variety of tissues including intestine (Wu et al., 2014), heart (Mohammadipoor et al., 2016; Shi et al., 2014; Westberg et al., 2007a), lung (Huang et al., 2015b; Tang et al., 2014), kidney (Huang et al., 2012; Huang et al., 2014; Huang et al., 2015a; Liu et al., 2016; Pan et al., 2015), cerebral neurons (Durukan Tolvanen et al., 2013; Westberg et al., 2007b; Zhang et al., 2000), retinal photoreceptors (Roddy et al., 2012), and retinal ganglion cells (Kim et al., 2013). Cellular protective functions of STC-1 have been attributed to its ability to reduce apoptosis (Huang et al., 2014; Kim et al., 2013; Tang et al., 2014), oxidative stress (Huang et al., 2012; Huang et al., 2015b; Kim et al., 2013; Liu et al., 2016; Nguyen et al., 2009; Roddy et al., 2012; Shi et al., 2014; Tang et al., 2014; Wu et al., 2014), and inflammation (Kanellis

et al., 2004; Mohammadipoor et al., 2016; Tang et al., 2014; Wang et al., 2009), which are all pathways involved in RD (Ding et al., 2009). We recently demonstrated that intravitreal injection(s) of recombinant human STC-1 delayed photoreceptor degeneration in the rapidly degenerating S334ter-3 rhodopsin transgenic rat and in the Royal College of Surgeons rat (Roddy et al., 2012). The reduction in photoreceptor loss was attributed in part to the reduction of oxidation damage products following the induction of mitochondrial uncoupling protein-2 (UCP-2), which uncouples oxidative phosphorylation leading to a decrease in the production of endogenous free radicals (Wang et al., 2009). Photoreceptor viability as assessed by quantitative real time-PCR (qPCR) of photoreceptor specific genes indicates that it reaches its nadir at approximately 2 weeks in the S334ter-3 and 7 weeks in the RCS rat, indicating the relatively acute nature of the degeneration of both models (Roddy et al., 2012).

In the present study, to explore the longer-term capability of photoreceptor rescue by STC-1, we used P23H-1 and S334ter-4 rhodopsin transgenic rats with more slowly evolving RDs compared to the S334ter-3 and RCS rats used in our previous study (Roddy et al., 2012). The P23H-1 transgenic rats contain a single amino acid substitution at codon 23 (P23H) which causes protein misfolding and subsequent ubiquitin-proteosome mediated degradation (Orhan et al., 2015), while the S334ter-4 transgenic rats express rhodopsin bearing a termination codon at residue 334 that causes abnormal protein sorting in photoreceptors and subsequent endoplasmic reticulum stress (Green et al., 2000; Lee et al., 2003; Shinde et al., 2012). All procedures with the animals followed the guidelines of the National Institutes of Health for the care and use of laboratory animals.

To achieve sustained delivery of STC-1 in these transgenic rat models of RD, we generated an adeno-associated virus (AAV) construct that enabled long-term expression of STC-1 (AAV-STC-1). AAV-STC-1 was designed to maintain the signal peptide, incorporate a FLAG tag at the C-terminus, and express human STC-1 under the control of a retinal ganglion cell targeting promoter, human synapsin 1 (hSYN1). The vector was packaged in capsid-modified AAV2 vector containing 3 surface-exposed tyrosine to phenylalanine mutations (AAV2-tripleYF) (Fig. 1A). P23H-1 and S334ter-4 heterozygote rhodopsin transgenic rats were treated with a single intravitreal injection of 2 μL of AAV-STC-1 using a 32g beveled needle at postnatal day 10 (P10) and sacrificed at P120 for tissue analysis. The contralateral eye served as an uninjected (UI) control, which shows no rescue from either the injection injury or the AAV alone (LaVail and colleagues, unpublished observations). Tissues were prepared for histologic analysis, and the outer nuclear layer (ONL) thickness was quantified by taking a total of 54 measurements from the superior and inferior hemispheres of each eye as previously described (Lewin et al., 1998; Roddy et al., 2012). In a cohort of animals, electroretinography was performed as previously described (Lewin et al., 1998; Roddy et al., 2012) at P120. Whole rat retinas were harvested and RNA was isolated and processed as previously described for microarray and qPCR (Roddy et al., 2012). TaqMan probes used were Rn00591060_m1 (Gpnmb), Rn00561387_m1 (Hmox), Rn00583001_g1 (Hspb1), Rn01508544_g1 (Nupr1), Rn00709999_m1 (Serpinf1), Rn01754856_m1 (UCP-2), and Rn01492482_m1 (Usp18) (Thermofisher, Waltham, MA). Relative expression values were determined after normalization to 18s RNA and subsequently to the uninjected fellow eye. Protein was isolated from whole rat retina as

previously described (Roddy et al., 2012), and western blots were performed and quantified as previously described (Roy Chowdhury et al., 2017). Primary antibodies used were M2 anti-FLAG (Sigma Aldrich, St Louis, MO) and anti-GAPDH (ab181602, Abcam, Cambridge MA), and secondary antibody used was horseradish peroxidase conjugated anti-mouse (GE Healthcare, Piscataway, NJ). Relative expression values were determined by densitometry with normalization to GAPDH and subsequently the uninjected fellow eye. A paired, 2-tailed Student's t-test was used for statistical analysis.

In the P23H-1 rat, STC-1 gene expression was induced 38 ± 16-fold compared to the UI control eye (n=6, $*P<0.05$, Fig. 1B) while in the S334ter-4 rat, STC-1 gene expression was induced 292 ± 107-fold compared to the UI control eye (n=5, Fig. 1B, $***P<0.005$). At the protein level, FLAG was induced 3.8 ± 1.7-fold in the P23H-1 rat (n=5, P=0.1, Fig. 1B), while in the S334ter-4 rat FLAG was induced 3.4 ± 1.2-fold (n=5, P=0.4, Fig. 1B). A representative blot shows FLAG expression in AAV-STC-1 injected and UI control eyes in both the P23H-1 and S334ter-4 rat (Fig. 1C).

P23H-1 rhodopsin transgenic rats injected at P10 with AAV-STC-1 showed significant photoreceptor preservation as assessed by ONL thickness compared to the UI control eye (n=7, $*P<0.05$, Fig. 1D). Retinal spidergram analysis showed increased ONL thickness in superior and inferior retina (Fig. 1E). Histologic analysis revealed a thicker ONL and healthier photoreceptor inner and outer segments in eyes treated with AAV-STC-1 compared to those of the contralateral control eyes (Fig. 1F). Electroretinographic analysis in P23H-1 animals (n=5) injected with STC-1 showed significantly increased scotopic b-wave ($***P<0.005$, Fig. 1G), and photopic b-wave ($*P<0.05$, Fig. 1H). The scotopic a-wave was also increased, but did not reach statistical significance.

S334ter-4 rhodopsin transgenic rats injected at P10 with AAV-STC-1 showed significant photoreceptor preservation as assessed by ONL thickness compared to the UI control eye (n=8, $***P<0.005$, Fig. 1I). Retinal spidergram analysis revealed increased ONL thickness in superior and inferior retina (Fig. 1J). Histologic analysis revealed a thicker ONL and healthier photoreceptor inner and outer segments in eyes treated with AAV-STC-1 compared to those of the contralateral control eyes (Fig. 1K). No significant change in ERG response amplitudes was observed in S334ter-4 animals treated with AAV-STC-1 at P120 (data not shown).

To assess molecular changes with AAV-STC-1 treatment, we isolated total RNA from AAV-STC-1 injected and control P23H-1 (n=6 paired RNA samples, n=1 paired samples selected for microarray) and S334ter-4 (n=5 paired RNA samples, n=1 paired samples selected for microarray) rat retinas (P120) and used Affymetrix microarrays and bioinformatics analysis to identify differentially regulated genes. Following overexpression of STC-1 in the P23H-1 rat model, 133 genes were upregulated ≥2-fold and 207 were downregulated ≥2-fold. Following overexpression of STC-1 in the S334ter-4 model, 385 genes were upregulated ≥2-fold and 518 were downregulated ≥2-fold. 62 common genes were upregulated ≥2-fold and 9 common genes were downregulated ≥2-fold in both P23H-1 and S334ter-4 models (Fig. 2A). From these commonly upregulated genes, selected genes of interest with known anti-apoptotic, anti-oxidant, or neuroprotective functions were selected for confirmatory analysis

with qPCR (Fig. 2B). Additionally, though not identified by microarray analysis, UCP-2 was also selected for confirmatory analysis as we previously identified this gene as upregulated in the retina after STC-1 treatment (Roddy et al., 2012). In the S334ter-4 model, multiple genes including Gpnmb, Hmox, Hspb1 (Hsp27), Nupr, Serpinf1 (PEDF), UCP-2, and USP18 were confirmed to be significantly upregulated following overexpression of STC-1 (Fig. 2C). Interestingly these same genes of interest were not significantly upregulated in the P23H-1 rat by qPCR (data not shown).

The initial reports of STC-1, first called teleocalcin, described its function in mineral metabolism in bony fish (Gerritsen and Wagner, 2005) in the 1980s (Wagner et al., 1986). Shortly after its identification in mammals (Wagner et al., 1995), it was described as a neuroprotective agent in cerebral neurons after ischemic challenge (Zhang et al., 2000). STC-1 has recently been found to have multiple functions in the eye. Its neuroprotective properties were first reported in photoreceptors (Roddy et al., 2012) and later in retinal ganglion cells (Kim et al., 2013). More recently it was found that STC-1 is expressed by trabecular meshwork and Schlemm canal cells and is a key molecule necessary for the ocular hypotensive activity of the prostaglandin analog, latanoprost (Roddy et al., 2017). Additionally, when used as a stand-alone therapy, topical administration of STC-1 reduced intraocular pressure in vivo (Roddy et al., 2017).

In the present study, we found that STC-1 overexpression via AAV transduction reduced photoreceptor degeneration when assessed by ONL measurements at P120 in both the S334ter-4 and P23H-1 models. Scotopic and photopic ERG response amplitudes were significantly increased in AAV-STC-1 treated eyes compared to control eyes in the P23H-1 model at P120; however, no significant change was seen in the S334ter-4 model in treated compared to control eyes. Reasons for disparity in the histologic and functional rescue in the S334ter-4 are unclear but may be due to the timing of the assay compared to the course of degeneration of each model. ERG responses in the P23H-1 rats hit their nadir at approximately 6 months of age (Orhan et al., 2015), while it is about 8 weeks in the S334ter-4 rats (Glybina et al., 2010), and perhaps we missed the treatment window of ability to detect a functional (ERG) change in the S334ter-4 as the disease progressed, particularly since the ERG wave amplitudes are already greatly reduced by P84 (Glybina et al., 2010).

There was additional disparity in the amount of STC-1 gene expression as well as global gene expression changes. In the P23H-1 eyes, there was a 38 ± 16-fold induction in STC-1 gene expression with AAV-STC-1 treatment, while in the S334ter-4 eyes, there was a 292 ± 107-fold induction at P120, while the level of STC-1 protein expression was similar in both models as assessed by FLAG. Two important points must be considered. The first is the variation in STC-1 gene expression within each model. There were some animals in each model that showed almost no upregulated expression of STC-1 indicating perhaps an injection that did not deliver adequate amount of AAV-STC-1 to the eye. This corresponds with a limited number of animals in our study that did not exhibit histologic rescue as previously mentioned (see Fig. 1 legend). The second is that the S334ter-4 eyes showed higher level of gene expression of STC-1 than the P23H-1 eyes. Since the STC-1 is driven by a retinal ganglion cell promoter, one possibility is related to loss of that cell-type over time. In the P23H model, the retinal ganglion cells and nerve fiber layer thins approximately

30% from 1 month of age to 3–6 months of age (Orhan et al., 2015), which could result in decreased expression of STC-1. The inner retina of S334ter-4 rats is less well characterized. Additionally, since the levels of protein expression were similar, there may be differences in translation since the S334ter-4 is characterized by ER stress (Green et al., 2000; Lee et al., 2003; Shinde et al., 2012). Additionally, western blot analysis from whole retina may underestimate the STC-1 protein product due to it being a secreted peptide hormone (Gerritsen and Wagner, 2005). Microarray analysis revealed differentially regulated genes that were common to both models after treatment with AAV-STC-1. Interestingly, confirmatory qPCR revealed significant changes in these genes only in the S334ter-4 model. The reason for the disparity in gene expression between the two models may be related to the lower AAV-STC-1 expression in the P23H-1 at the time-point of the assay (P120), differences in the rate of degeneration in each model, or separate mechanisms of therapeutic action by STC-1 in each model.

In summary, we demonstrate the successful delivery of STC-1 using an AAV vector in two different rat models of RD that resulted in a delay in photoreceptor degeneration without evidence of negative side effects. Thus, STC-1 may be a useful neuroprotective agent for long-term use via AAV delivery or with repeated intravitreal injections in patients with inherited and age-related RDs.

Acknowledgments

This work was funded in part by NIH research grants EY001919, EY006842, P30EY002162 (MML), P30EY021721 (WWH) and EY021727 (MPF); Unrestricted Awards from Research to Prevent Blindness to UCSF, University of Florida, and Mayo Clinic; the Foundation Fighting Blindness (MML, WWH), That Man May See, Inc. (MML) and the Mayo Foundation (GWR). WWH and the University of Florida have a financial interest in the use of AAV therapies, WWH owns equity in and is a consultant for AGTC and has a conflict of interest to the extent that this work potentially increases their financial interests. The other authors declare that no conflict of interest exists.

References

Bachner D, Schroder D, Gross G. mRNA expression of the murine glycoprotein (transmembrane) nmb (Gpnmb) gene is linked to the developing retinal pigment epithelium and iris. Brain Res Gene Expr Patterns. 2002; 1:159–165. [PubMed: 12638126]

Cottet S, Schorderet DF. Mechanisms of apoptosis in retinitis pigmentosa. Curr Mol Med. 2009; 9:375–383. [PubMed: 19355918]

Cuenca N, Fernandez-Sanchez L, Campello L, Maneu V, De la Villa P, Lax P, Pinilla I. Cellular responses following retinal injuries and therapeutic approaches for neurodegenerative diseases. Prog Retin Eye Res. 2014; 43:17–75. [PubMed: 25038518]

Ding X, Patel M, Chan CC. Molecular pathology of age-related macular degeneration. Prog Retin Eye Res. 2009; 28:1–18. [PubMed: 19026761]

Doonan F, Cotter TG. Apoptosis: a potential therapeutic target for retinal degenerations. Curr Neurovasc Res. 2004; 1:41–53. [PubMed: 16181065]

Dunaief JL, Dentchev T, Ying GS, Milam AH. The role of apoptosis in age-related macular degeneration. Arch Ophthalmol. 2002; 120:1435–1442. [PubMed: 12427055]

Durukan Tolvanen A, Westberg JA, Serlachius M, Chang AC, Reddel RR, Andersson LC, Tatlisumak T. Stanniocalcin 1 is important for poststroke functionality, but dispensable for ischemic tolerance. Neuroscience. 2013; 229:49–54. [PubMed: 23159313]

Elahy M, Baindur-Hudson S, Cruzat VF, Newsholme P, Dass CR. Mechanisms of PEDF-mediated protection against reactive oxygen species damage in diabetic retinopathy and neuropathy. J Endocrinol. 2014; 222:R129–139. [PubMed: 24928938]

Gerritsen ME, Wagner GF. Stanniocalcin: no longer just a fish tale. Vitam Horm. 2005; 70:105–135. [PubMed: 15727803]

Glybina IV, Kennedy A, Ashton P, Abrams GW, Iezzi R. Intravitreous delivery of the corticosteroid fluocinolone acetonide attenuates retinal degeneration in S334ter-4 rats. Invest Ophthalmol Vis Sci. 2010; 51:4243–4252. [PubMed: 20220055]

Goldmann T, Zeller N, Raasch J, Kierdorf K, Frenzel K, Ketscher L, Basters A, Staszewski O, Brendecke SM, Spiess A, Tay TL, Kreutz C, Timmer J, Mancini GM, Blank T, Fritz G, Biber K, Lang R, Malo D, Merkler D, Heikenwalder M, Knobeloch KP, Prinz M. USP18 lack in microglia causes destructive interferonopathy of the mouse brain. EMBO J. 2015; 34:1612–1629. [PubMed: 25896511]

Green ES, Menz MD, LaVail MM, Flannery JG. Characterization of rhodopsin mis-sorting and constitutive activation in a transgenic rat model of retinitis pigmentosa. Invest Ophthalmol Vis Sci. 2000; 41:1546–1553. [PubMed: 10798675]

Grochot-Przeczek A, Dulak J, Jozkowicz A. Haem oxygenase-1: non-canonical roles in physiology and pathology. Clin Sci (Lond). 2012; 122:93–103. [PubMed: 21992109]

Hamidi T, Algul H, Cano CE, Sandi MJ, Molejon MI, Riemann M, Calvo EL, Lomberk G, Dagorn JC, Weih F, Urrutia R, Schmid RM, Iovanna JL. Nuclear protein 1 promotes pancreatic cancer development and protects cells from stress by inhibiting apoptosis. J Clin Invest. 2012; 122:2092–2103. [PubMed: 22565310]

Huang L, Belousova T, Chen M, DiMattia G, Liu D, Sheikh-Hamad D. Overexpression of stanniocalcin-1 inhibits reactive oxygen species and renal ischemia/reperfusion injury in mice. Kidney Int. 2012; 82:867–877. [PubMed: 22695329]

Huang L, Belousova T, Pan JS, Du J, Ju H, Lu L, Zhang P, Truong LD, Nuotio-Antar A, Sheikh-Hamad D. AKI after conditional and kidney-specific knockdown of stanniocalcin-1. J Am Soc Nephrol. 2014; 25:2303–2315. [PubMed: 24700878]

Huang L, Lou Y, Ju H, Zhang L, Pan JS, Ross A, Sun Y, Truong LD, Sheikh-Hamad D. Severe Nephrotoxic Nephritis following Conditional and Kidney-Specific Knockdown of Stanniocalcin-1. PLoS One. 2015a; 10:e0138440. [PubMed: 26393521]

Huang L, Zhang L, Ju H, Li Q, Pan JS, Al-Lawati Z, Sheikh-Hamad D. Stanniocalcin-1 inhibits thrombin-induced signaling and protects from bleomycin-induced lung injury. Sci Rep. 2015b; 5:18117. [PubMed: 26640170]

Kanellis J, Bick R, Garcia G, Truong L, Tsao CC, Etemadmoghadam D, Poindexter B, Feng L, Johnson RJ, Sheikh-Hamad D. Stanniocalcin-1, an inhibitor of macrophage chemotaxis and chemokinesis. Am J Physiol Renal Physiol. 2004; 286:F356–362. [PubMed: 14570698]

Katai N, Kikuchi T, Shibuki H, Kuroiwa S, Arai J, Kurokawa T, Yoshimura N. Caspaselike proteases activated in apoptotic photoreceptors of Royal College of Surgeons rats. Invest Ophthalmol Vis Sci. 1999; 40:1802–1807. [PubMed: 10393051]

Katai N, Yanagidaira T, Senda N, Murata T, Yoshimura N. Expression of c-Jun and Bcl-2 family proteins in apoptotic photoreceptors of RCS rats. Jpn J Ophthalmol. 2006; 50:121–127. [PubMed: 16604387]

Kim SJ, Ko JH, Yun JH, Kim JA, Kim TE, Lee HJ, Kim SH, Park KH, Oh JY. Stanniocalcin-1 protects retinal ganglion cells by inhibiting apoptosis and oxidative damage. PLoS One. 2013; 8:e63749. [PubMed: 23667669]

LaVail MM, Yasumura D, Matthes MT, Lau-Villacorta C, Unoki K, Sung C-H, Steinberg RH. Protection of mouse photoreceptors by survival factors in retinal degenerations. Invest Ophthalmol Vis Sci. 1998; 39:592–602. [PubMed: 9501871]

Lee D, Geller S, Walsh N, Valter K, Yasumura D, Matthes M, LaVail M, Stone J. Photoreceptor degeneration in Pro23His and S334ter transgenic rats. Advances in experimental medicine and biology. 2003; 533:297–302. [PubMed: 15180276]

Lewin AS, Drenser KA, Hauswirth WW, Nishikawa S, Yasumura D, Flannery JG, LaVail MM. Ribozyme rescue of photoreceptor cells in a transgenic rat model of autosomal dominant retinitis pigmentosa. Nat Med. 1998; 4:967–971. [PubMed: 9701253]

Liu D, Shang H, Liu Y. Stanniocalcin-1 Protects a Mouse Model from Renal Ischemia-Reperfusion Injury by Affecting ROS-Mediated Multiple Signaling Pathways. Int J Mol Sci. 2016:17.

Manini I, Sgorbissa A, Potu H, Tomasella A, Brancolini C. The DeISGylase USP18 limits TRAIL-induced apoptosis through the regulation of TRAIL levels: Cellular levels of TRAIL influences responsiveness to TRAIL-induced apoptosis. Cancer Biol Ther. 2013; 14:1158–1166. [PubMed: 24153058]

Mattiasson G, Shamloo M, Gido G, Mathi K, Tomasevic G, Yi S, Warden CH, Castilho RF, Melcher T, Gonzalez-Zulueta M, Nikolich K, Wieloch T. Uncoupling protein-2 prevents neuronal death and diminishes brain dysfunction after stroke and brain trauma. Nat Med. 2003; 9:1062–1068. [PubMed: 12858170]

Mohammadipoor A, Lee RH, Prockop DJ, Bartosh TJ. Stanniocalcin-1 attenuates ischemic cardiac injury and response of differentiating monocytes/macrophages to inflammatory stimuli. Transl Res. 2016; 177:127–142. [PubMed: 27469269]

Motterlini R, Foresti R. Heme oxygenase-1 as a target for drug discovery. Antioxid Redox Signal. 2014; 20:1810–1826. [PubMed: 24180608]

Nguyen A, Chang AC, Reddel RR. Stanniocalcin-1 acts in a negative feedback loop in the prosurvival ERK1/2 signaling pathway during oxidative stress. Oncogene. 2009; 28:1982–1992. [PubMed: 19347030]

O'Reilly AM, Currie RW, Clarke DB. HspB1 (Hsp 27) expression and neuroprotection in the retina. Mol Neurobiol. 2010; 42:124–132. [PubMed: 20514530]

Orhan E, Dalkara D, Neuille M, Lechauve C, Michiels C, Picaud S, Leveillard T, Sahel JA, Naash MI, Lavail MM, Zeitz C, Audo I. Genotypic and phenotypic characterization of P23H line 1 rat model. PLoS One. 2015; 10:e0127319. [PubMed: 26009893]

Pan JS, Huang L, Belousova T, Lu L, Yang Y, Reddel R, Chang A, Ju H, DiMattia G, Tong Q, Sheikh-Hamad D. Stanniocalcin-1 inhibits renal ischemia/reperfusion injury via an AMP-activated protein kinase-dependent pathway. J Am Soc Nephrol. 2015; 26:364–378. [PubMed: 25012175]

Roddy GW, Rosa RH Jr, Oh JY, Ylostalo JH, Bartosh TJ Jr, Choi H, Lee RH, Yasumura D, Ahern K, Nielsen G, Matthes MT, LaVail MM, Prockop DJ. Stanniocalcin-1 rescued photoreceptor degeneration in two rat models of inherited retinal degeneration. Mol Ther. 2012; 20:788–797. [PubMed: 22294148]

Roddy GW, Viker KB, Winkler NS, Bahler CK, Holman BH, Sheikh-Hamad D, Roy Chowdhury U, Stamer WD, Fautsch MP. Stanniocalcin-1 is an ocular hypotensive agent and a downstream effector molecule that is necessary for the intraocular pressure-lowering effects of latanoprost. Invest Ophthalmol Vis Sci. 2017; 58:2715–2724. [PubMed: 28538979]

Roy Chowdhury U, Dosa PI, Fautsch MP. ATP sensitive potassium channel openers: A new class of ocular hypotensive agents. Exp Eye Res. 2017; 158:85–93. [PubMed: 27130546]

Scholl HP, Strauss RW, Singh MS, Dalkara D, Roska B, Picaud S, Sahel JA. Emerging therapies for inherited retinal degeneration. Sci Transl Med. 2016; 8:368rv366.

Shi X, Wang J, Qin Y. Recombinant adeno-associated virus-delivered hypoxia-inducible stanniocalcin-1 expression effectively inhibits hypoxia-induced cell apoptosis in cardiomyocytes. J Cardiovasc Pharmacol. 2014; 64:522–529. [PubMed: 25490418]

Shinde VM, Sizova OS, Lin JH, LaVail MM, Gorbatyuk MS. ER stress in retinal degeneration in S334ter Rho rats. PLoS One. 2012; 7:e33266. [PubMed: 22432009]

Tanaka H, Shimazawa M, Kimura M, Takata M, Tsuruma K, Yamada M, Takahashi H, Hozumi I, Niwa J, Iguchi Y, Nikawa T, Sobue G, Inuzuka T, Hara H. The potential of GPNMB as novel neuroprotective factor in amyotrophic lateral sclerosis. Sci Rep. 2012; 2:573. [PubMed: 22891158]

Tang SE, Wu CP, Wu SY, Peng CK, Perng WC, Kang BH, Chu SJ, Huang KL. Stanniocalcin-1 ameliorates lipopolysaccharide-induced pulmonary oxidative stress, inflammation, and apoptosis in mice. Free Radic Biol Med. 2014; 71:321–331. [PubMed: 24685991]

Wagner GF, Guiraudon CC, Milliken C, Copp DH. Immunological and biological evidence for a stanniocalcin-like hormone in human kidney. Proc Natl Acad Sci U S A. 1995; 92:1871–1875. [PubMed: 7892193]

Wagner GF, Hampong M, Park CM, Copp DH. Purification, characterization, and bioassay of teleocalcin, a glycoprotein from salmon corpuscles of Stannius. Gen Comp Endocrinol. 1986; 63:481–491. [PubMed: 3557071]

Wang Y, Huang L, Abdelrahim M, Cai Q, Truong A, Bick R, Poindexter B, Sheikh-Hamad D. Stanniocalcin-1 suppresses superoxide generation in macrophages through induction of mitochondrial UCP2. Journal of leukocyte biology. 2009; 86:981–988. [PubMed: 19602668]

Westberg JA, Serlachius M, Lankila P, Andersson LC. Hypoxic preconditioning induces elevated expression of stanniocalcin-1 in the heart. Am J Physiol Heart Circ Physiol. 2007a; 293:H1766–1771. [PubMed: 17573464]

Westberg JA, Serlachius M, Lankila P, Penkowa M, Hidalgo J, Andersson LC. Hypoxic preconditioning induces neuroprotective stanniocalcin-1 in brain via IL-6 signaling. Stroke. 2007b; 38:1025–1030. [PubMed: 17272771]

Wu LM, Guo R, Hui L, Ye YG, Xiang JM, Wan CY, Zou M, Ma R, Sun XZ, Yang SJ, Guo DZ. Stanniocalcin-1 protects bovine intestinal epithelial cells from oxidative stress-induced damage. J Vet Sci. 2014; 15:475–483. [PubMed: 24962416]

Xu GZ, Li WW, Tso MO. Apoptosis in human retinal degenerations. Trans Am Ophthalmol Soc. 1996; 94:411–430. discussion 430–411. [PubMed: 8981707]

Yu DY, Cringle S, Valter K, Walsh N, Lee D, Stone J. Photoreceptor death, trophic factor expression, retinal oxygen status, and photoreceptor function in the P23H rat. Invest Ophthalmol Vis Sci. 2004; 45:2013–2019. [PubMed: 15161870]

Zhang K, Lindsberg PJ, Tatlisumak T, Kaste M, Olsen HS, Andersson LC. Stanniocalcin: A molecular guard of neurons during cerebral ischemia. Proc Natl Acad Sci U S A. 2000; 97:3637–3642. [PubMed: 10725397]

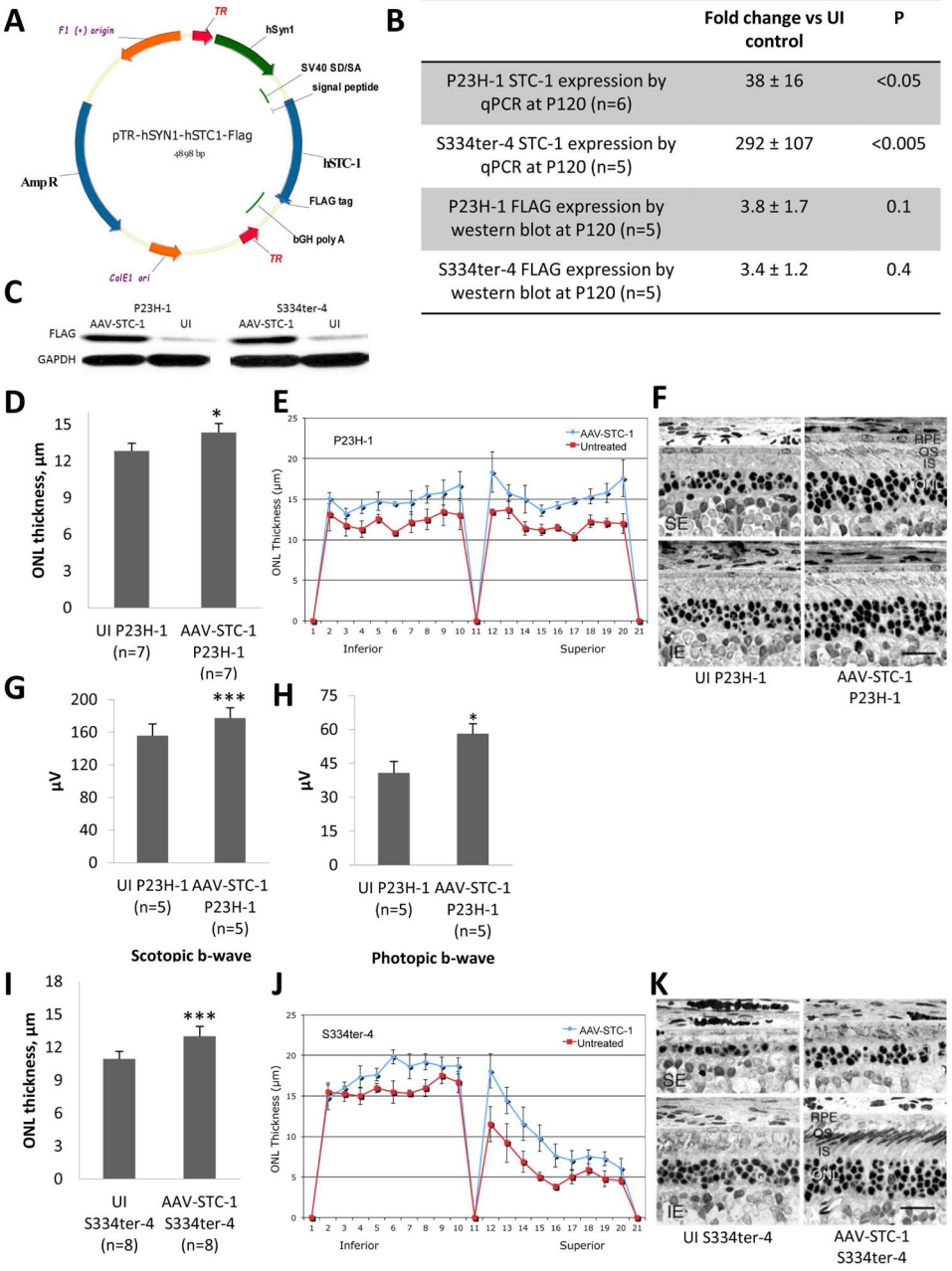

	Fold change vs UI control	P
P23H-1 STC-1 expression by qPCR at P120 (n=6)	38 ± 16	<0.05
S334ter-4 STC-1 expression by qPCR at P120 (n=5)	292 ± 107	<0.005
P23H-1 FLAG expression by western blot at P120 (n=5)	3.8 ± 1.7	0.1
S334ter-4 FLAG expression by western blot at P120 (n=5)	3.4 ± 1.2	0.4

Fig. 1.

AAV-STC-1 construct and anatomic and functional rescue with AAV-STC-1. (A) AAV-STC-1 construct. Construct was designed to 1) incorporate a FLAG tag at the C-terminus, 2) maintain the signal peptide and 3) express hSTC-1 under the control of a retinal ganglion cell targeting promoter, human synapsin 1 (hSYN1). Vector was packaged in capsid modified AAV2 vector containing 3 surface-exposed tyrosine to phenylalanine mutations (AAV2-tripleYF). (B) After injection of AAV-STC-1 at P10, STC-1 gene expression was induced 38-fold in the P23H-1 rat (n=6, mean ± SEM, **P*<0.05) and 292-fold in the S334ter-4 rat (n=5, mean ± SEM, ****P*<0.005) at P120 while FLAG protein expression was

induced 3.8-fold in the P23H-1 rat (n=5, P=0.1, Fig. 1B), and 3.4-fold in the S334ter-4 rat (n=5, P=0.4, Fig. 1B). (C) A representative western blot showing FLAG expression in AAV-STC-1 and UI retinas from P23H-1 and S334ter-4 rats. (D) At P120, AAV-STC-1 significantly improved ONL thickness of treated eyes of P23H-1 rats (n=7, mean ± SEM, $*P<0.05$). Note that this level of statistical significance was reached despite the fact that 3 of the 7 rats showed little rescue, presumably due to unsuccessful injections that occasionally occur with such experiments (LaVail et al., 1998) and variation of STC-1 overexpression between animals. (E) Spidergram reveals increased ONL thickness in superior and inferior retina of treated P23H-1 rats (n=3 showing greatest rescue; mean ± SEM; $*P<0.05$). (F) Histologic analysis revealed a thicker ONL and healthier photoreceptor inner (IS) and outer segments (OS) in eyes treated with AAV-STC-1 compared to those of the contralateral uninjected (UI) control eyes. The UI eyes are shown in the left column, and the injected eyes are shown on the right; the top row is taken from the superior equatorial (SE) retina, and the bottom row is taken from the inferior equatorial (IE) retina. Magnification bar = 25 μm. (G) At P120, scotopic (n=5, mean ± SEM, $**P<0.005$) and (H) photopic (n=5, mean ± SEM, $*P<0.05$) b-wave ERG response amplitudes were significantly increased in AAV-STC-1 treated P23H-1 animals. (I) At P120, AAV-STC-1 significantly improved ONL thickness of S334ter-4 rats (n=8, mean ± SEM, $***P<0.005$). Note that this level of statistical significance was reached despite the fact that 2 of the 8 rats showed little or no rescue, presumably due to unsuccessful injections. (J) Spidergram reveals increased ONL thickness in superior and inferior retina in treated eyes of S334ter-4 rats (n=5 showing the greatest rescue; mean ± SEM; $**P<0.01$). (K) Histologic analysis shows a thicker ONL and healthier photoreceptor inner and outer segments in S334ter-4 eyes treated with AAV-STC-1 compared to those of the contralateral uninjected (UI) control eye. Light micrographs represent the most extensive rescue in this cohort. The labels are the same as in (F).

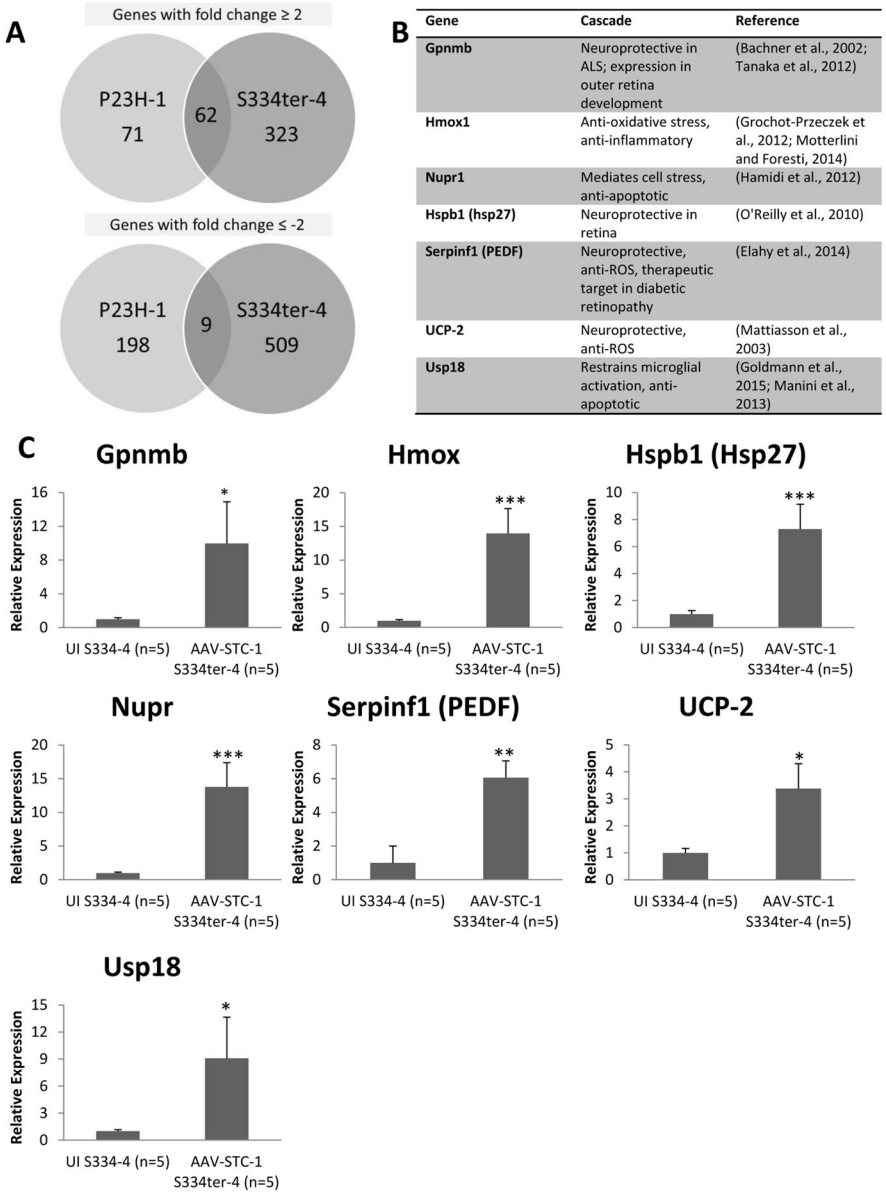

Gene	Cascade	Reference
Gpnmb	Neuroprotective in ALS; expression in outer retina development	(Bachner et al., 2002; Tanaka et al., 2012)
Hmox1	Anti-oxidative stress, anti-inflammatory	(Grochot-Przeczek et al., 2012; Motterlini and Foresti, 2014)
Nupr1	Mediates cell stress, anti-apoptotic	(Hamidi et al., 2012)
Hspb1 (hsp27)	Neuroprotective in retina	(O'Reilly et al., 2010)
Serpinf1 (PEDF)	Neuroprotective, anti-ROS, therapeutic target in diabetic retinopathy	(Elahy et al., 2014)
UCP-2	Neuroprotective, anti-ROS	(Mattiasson et al., 2003)
Usp18	Restrains microglial activation, anti-apoptotic	(Goldmann et al., 2015; Manini et al., 2013)

Fig. 2.

Gene expression changes following treatment with AAV-STC-1. (A) Microarray analysis was performed in the P23H-1 (n=1) and the S334ter-4 (n=1) models and revealed a cohort of genes upregulated in both models. In the P23H-1 model, 133 genes were upregulated ≥2-fold. In the S334ter-4 model, 385 genes were upregulated ≥2-fold. 62 common genes were upregulated ≥2-fold in both P23H-1 and S334ter-4 models. In the P23H-1 model, 207 genes were downregulated ≥2-fold. In the S334ter-4 model, 518 genes were downregulated ≥2-fold. 9 common genes were downregulated ≥2-fold in both P23H-1 and S334ter-4 models (B) Genes of interest based on their function that were upregulated ≥2-fold in both models by microarray were selected for further analysis by quantitative real-time PCR (qPCR).

Additionally, UCP-2 was also selected for further study. (C) qPCR revealed selected genes significantly upregulated (*P<0.05, **P<0.01, or ***P<0.005) in the S334ter-4 model (n=5).